JACS
JOURNAL OF THE AMERICAN CHEMICAL SOCIETY
pubs.acs.org/JACS
Article

Multiarm-Assisted Design of Dendron-like Degradable Ionizable Lipids Facilitates Systemic mRNA Delivery to the Spleen

Lulu Xue, Xinhong Xiong, Gan Zhao, William Molina-Arocho, Rohan Palanki, Zebin Xiao, Xuexiang Han, Il-Chul Yoon, Christian G. Figueroa-Espada, Junchao Xu, Ningqiang Gong, Qiangqiang Shi, Qinyuan Chen, Mohamad-Gabriel Alameh, Andrew E. Vaughan, Malay Haldar, Karin Wang, Drew Weissman, and Michael J. Mitchell*

Cite This: https://doi.org/10.1021/jacs.4c10265
Read Online

ABSTRACT: Lipid nanoparticles (LNPs) have emerged as pivotal vehicles for messenger RNA (mRNA) delivery to hepatocytes upon systemic administration and to antigen-presenting cells following intramuscular injection. However, achieving systemic mRNA delivery to non-hepatocytes remains challenging without the incorporation of targeting ligands such as antibodies, peptides, or small molecules. Inspired by comb-like polymeric architecture, here we utilized a multiarm-assisted design to construct a library of 270 dendron-like degradable ionizable lipids by altering the structures of amine heads and multiarmed tails for optimal mRNA delivery. Following in vitro high-throughput screening, a series of top-dendron-like LNPs with high transfection efficacy were identified. These dendron-like ionizable lipids facilitated greater mRNA delivery to the spleen in vivo compared to ionizable lipid analogs lacking dendron-like structure. Proteomic analysis of corona-LNP pellets showed enhancement of key protein clusters, suggesting potential endogenous targeting to the spleen. A lead dendron-like LNP formulation, 18−2−9b2, was further used to encapsulate Cre mRNA and demonstrated excellent genome modification in splenic macrophages, outperforming a spleen-tropic MC3/18PA LNP in the Ai14 mice model. Moreover, 18−2−9b2 LNP encapsulating therapeutic BTB domain and CNC homologue 1 (BACH1) mRNA exhibited proficient BACH1 expression and subsequent Spic downregulation in splenic red pulp macrophages (RPM) in a Spic-GFP transgene model upon intravenous administration. These results underscore the potential of dendron-like LNPs to facilitate mRNA delivery to splenic macrophages, potentially opening avenues for a range of mRNA-LNP therapeutic applications, including regenerative medicine, protein replacement, and gene editing therapies.

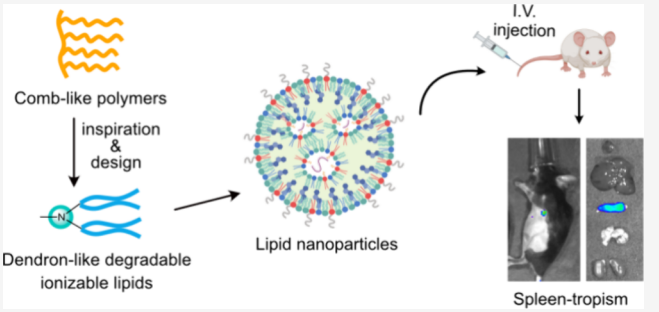

1. INTRODUCTION

Messenger RNA (mRNA)-based therapies have revolutionized treatments across a wide range of applications including vaccination, protein replacement therapy, cancer immunotherapy, and gene editing.[1−5] Among non-viral delivery systems, lipid nanoparticles (LNPs), comprised of an ionizable lipid, phospholipid, cholesterol, and poly(ethylene glycol) (PEG) lipid, have emerged as a promising platform for mRNA delivery.[6−9] Recently, the U.S. Food and Drug Administration (FDA) approved two COVID-19 mRNA vaccines delivered by LNPs to combat the global COVID-19 pandemic.[10−12] Simultaneously, LNP-mediated CRISPR-based gene therapies have showcased robust gene editing capabilities in clinical trials.[12,13] Within LNPs, the ionizable lipid plays a critical role in targeting specific tissues or cells and facilitating efficient translation.[14−21] Despite these advancements, the discontinuous vasculature of hepatic sinusoids results in preferential accumulation of mRNA-LNPs in the liver, confining transgene expression primarily to hepatic cells following systemic administration.[7,22,23] Therefore, there is a need to develop next-generation ionizable lipids capable of targeting extra-hepatic tissues for enhanced mRNA delivery.

The spleen is an immune cell-enriched tissue that plays a key role in maintaining the integrity of the blood, supporting the immune system, and contributing to hematopoiesis.[24−26] Various strategies have been explored to facilitate the delivery of mRNA-LNP to the spleen. One approach involves the incorporation of active targeting ligands, including proteins and peptides.[27−29] However, a limitation of this strategy is that active targeting often requires a multi-step manufacturing for

Received: July 27, 2024
Revised: September 20, 2024
Accepted: September 24, 2024
Published: January 1, 2025

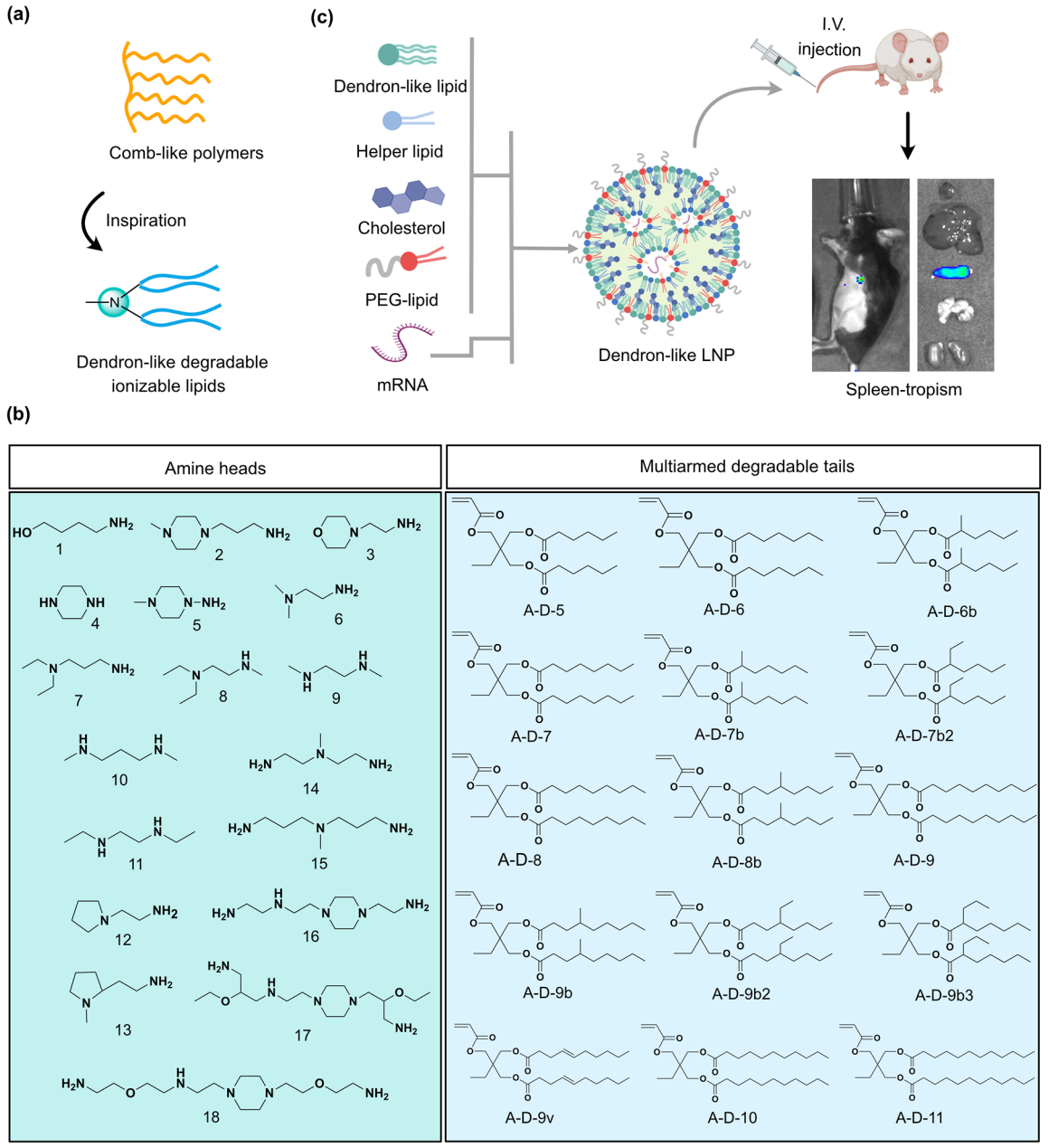

Figure 1. Multiarm-assisted design of dendron-like LNPs for mRNA delivery. (a) Comb-architecture polymer inspires the design of dendron-like degradable ionizable lipids. (b) Chemical structures of 18 amine cores (left) and 15 multiarmed degradable alkyl tails (right) for generating 270 dendron-like ionizable lipids used in this study. (c) Dendron-like LNPs were formulated via a microfluidic mixing device with dendron-like lipids, helper lipid, cholesterol, and PEG-lipid. The resulting dendron-like LNPs facilitate in vivo mRNA delivery to the spleen. I.V., intravenous.

LNP formulations, leading to poor reproducibility and translatability. Another approach includes the incorporation of anionic molecules as a fifth component into the standard four-component LNPs, such as 1,2-dioleoyl-*sn*-glycero-3-phosphate (18PA) and fatty acids, or as postmodification moieties within cationic polymer design.[22,23,30−33] However, the complex synthesis process of certain anionic lipids and the high negatively charge of the resulting LNPs limit the clinical application of spleen-selective mRNA-LNPs. Therefore, the development of ionizable lipids with intrinsic spleen tropism can enable simple and effective mRNA delivery to the spleen.[34−38]

Herein, we designed and synthesized a series of dendron-like degradable ionizable lipids and formulated a library of dendron-like LNPs to facilitate systemic delivery of mRNA to the spleen (Figure 1a). Initially, various acrylate-based tails were synthesized through a multiarm-assisted design and subsequently reacted with diverse amine cores to generate a library of 270 dendron-like ionizable lipids (Figure 1b). Following high-throughput in vitro screening in HeLa cells with firefly luciferase (FLuc)-encoding mRNA, several dendron-like LNPs exhibited superior protein expression compared to a gold standard LNP formulation. These top-performing dendron-like LNPs were further tested in vivo, demonstrating robust mRNA delivery to the spleen, in comparison with a counterpart lipid library lacking the dendron-like structure. A subsequent proteomic analysis of spleen-tropic 18−2−9b2 and MC3/18PA LNPs, as well as the

https://doi.org/10.1021/jacs.4c10265
J. Am. Chem. Soc. XXXX, XXX, XXX−XXX

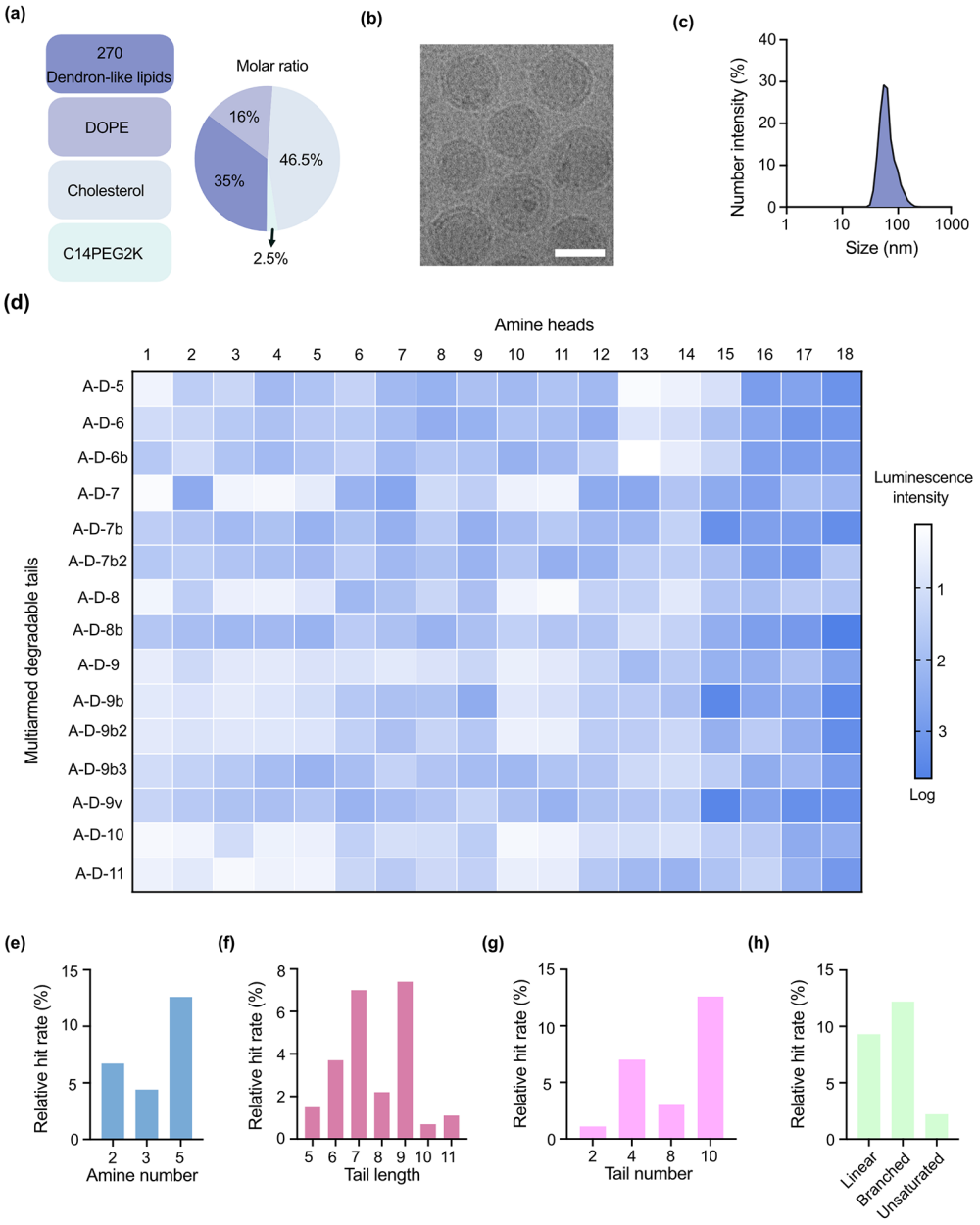

Figure 2. Structure−activity relationship (SAR) of dendron-like LNPs for FLuc mRNA delivery in vitro. (a) Dendron-like LNP formulation parameters. Dendron-like LNPs were formulated with one of 270 dendron-like lipids, DOPE, cholesterol, and C14PEG2K at a molar ratio of 35:16:46.5:2.5, respectively, for a total of 270 LNP formulations. (b) Representative cryogenic transmission electron microscopy (cryo-TEM) image of a dendron-like LNP morphology. Scale bar: 50 nm. (c) Representative hydrodynamic size of dendron-like LNP measured by DLS. (d) Heatmap of luciferase expression following treatment of HeLa cells with dendron-like LNPs (10 ng luciferase mRNA, n = 3 replicates). Relative luminescence unit (RLU) values of >200 were calculated as hits for hit rate calculation. (e) Relative hit rate of dendron-like LNPs with different secondary amine numbers. (f) Relative hit rate of dendron-like LNPs with different tail lengths. (g) Relative hit rate of dendron-like LNPs with different tail substitution numbers. (h) Relative hit rate of dendron-like LNPs with different tail architectures.

liver-tropic MC3 LNP, showed a significant difference in protein clusters. Notably, an enhanced Cluster 2 in 18−2−9b2 LNP-treated samples indicated endogenous spleen-targeting potential, with highly enriched markers such as Abcb6, Itga2, Itga2b, and Itgb2. Furthermore, reduced adsorption of apolipoprotein E (ApoE) and vitronectin (Vtn) in Cluster 1 from the pellet could potentially reduce the targeted delivery to the liver and lungs. Moreover, the lead dendron-like LNP, 18−2−9b2, encapsulating Cre mRNA demonstrated selective and effective genome modification of splenic macrophages, including red pulp macrophage (RPM) and marginal metallophilic macrophage (MMM), surpassing the performance of the spleen-tropic MC3/18PA formulation. Additionally, 18−2−9b2 encapsulating BTB domain and CNC homologue 1 (BACH1) mRNA exhibited robust BACH1 expression in RPM, resulting in the downregulation of Spic-GFP expression in a Spic-GFP transgene model. This study serves as a proof-of-concept demonstration of selective mRNA delivery to the spleen using a dendron-like architectural design of ionizable lipids. These results underscore the significance of structural evolution in developing novel ionizable lipids for organ-specific

https://doi.org/10.1021/jacs.4c10265
J. Am. Chem. Soc. XXXX, XXX, XXX−XXX

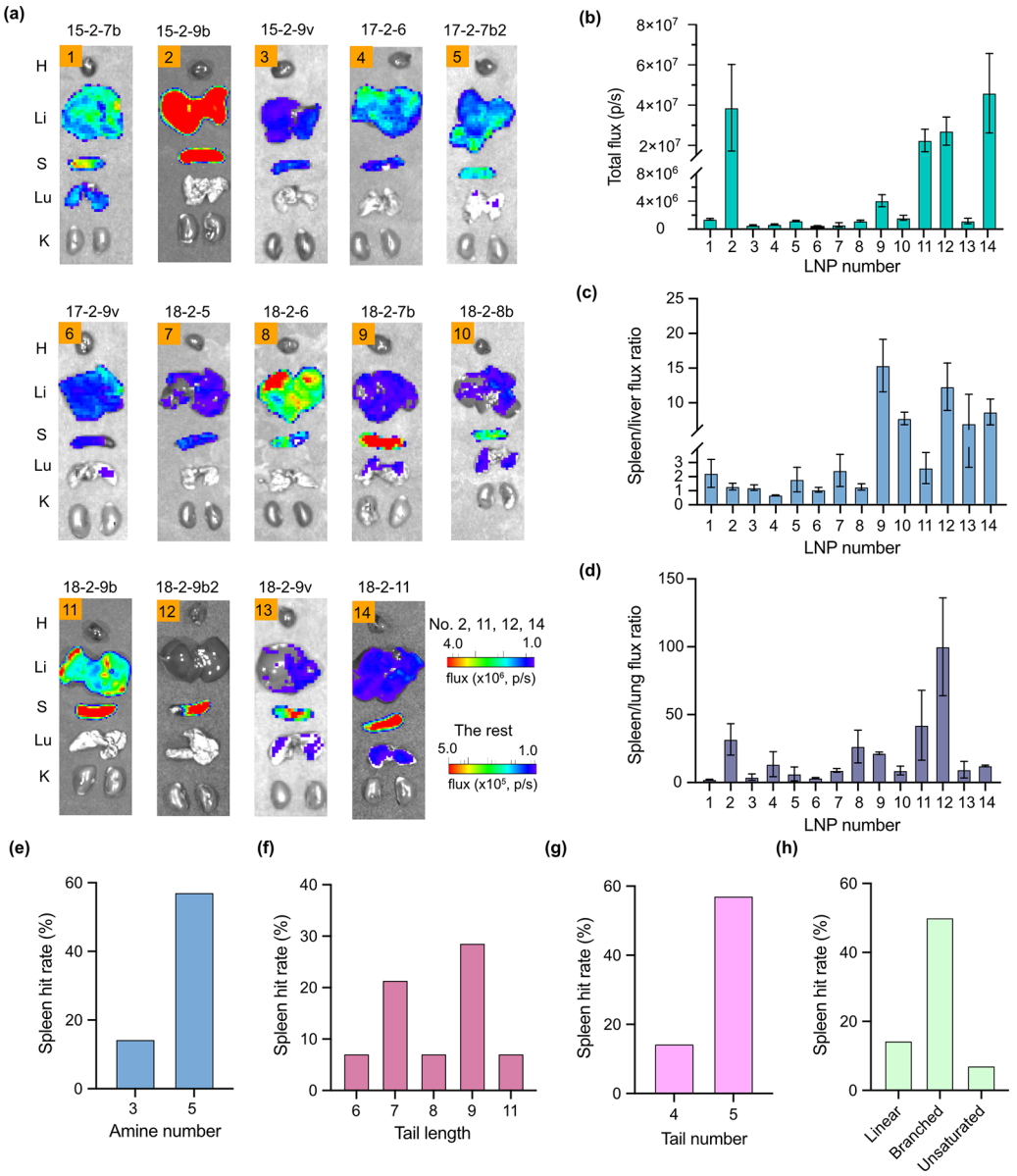

Figure 3. Dendron-like LNP-mediated in vivo delivery of mRNA to the spleen. (a) In vivo evaluation of 14 dendron-like LNPs encapsulating FLuc mRNA (dose: 0.1 mg/kg). Representative bioluminescence IVIS images of main organs taken 12h after systemic administration of dendron-like LNPs to C57BL/6J mice. H: heart; Li: liver; S: spleen; Lu: lungs; K: kidneys. (b) Quantified luciferase mRNA expression in the spleen from (a). (c, d) Spleen-targeting specificity was evaluated by calculating the relative luciferase expression of the spleen/liver (C) and spleen/lungs (d). (n = 3 mice) (e)−(h) Spleen-tropic hit rate calculation. Hits were defined as LNPs that enabled luminescence intensity greater than 1 × 10^6 p/s (total flux). Hit rate by amine number (e), tail length (f), tail substitution number (g), and tail morphologies (h).

delivery of mRNA for protein replacement therapy and gene editing applications.

2. RESULTS AND DISCUSSION

2.1. Multiarm-Assisted Design of Dendron-like Degradable Lipids. Comb-like polymers featuring densely grafted chains and tunable attributes, such as composition, shape, stiffness, and surface properties, have emerged as promising platforms for biomedical research, drug delivery, and diagnostic applications.[39−42] Notably, comb-architecture polymers have been increasingly utilized as effective vectors for RNA interference therapy, vaccination, and cancer therapy.[43−45] This architecture has previously been shown to direct delivery of genetic cargoes to the spleen using polymer systems[45]; however, the development of dendron-like structured ionizable lipids for nucleic acid delivery to the spleen remains challenging. This motivated us to explore a multiarmed and densely structured tail for incorporation into the ionizable lipid design. Initially, a series of multiarmed acrylate-based tails were synthesized through a two-step nucleophilic acyl substitution (Schemes S1 and S2). The reaction can occur under mild conditions with high yields (Figures S1−S16). Then, these multiarmed acrylate-based tails were reacted with various amine cores through a Michael addition reaction, yielding a library of 270 dendron-like degradable ionizable lipids.[46,47]

The resulting dendron-like lipid library with varying amine core structures, tail architectures, and tail substitution numbers were noted as X−2−Y, where "X" indicates the order of amine cores in this study and "2−Y" represents multiarmed

https://doi.org/10.1021/jacs.4c10265
J. Am. Chem. Soc. XXXX, XXX, XXX−XXX

degradable tails ("2" represents that there are 2 alkyl chains in each tail; "Y" represents the carbon number on each alkyl chain). These dendron-like lipids can be mixed with phospholipid, cholesterol, lipid-anchored polyethylene glycol, and mRNA using a microfluidic mixing device to generate LNPs with distinct physiochemical properties (Figure 1c).[14,48,49] This combinatorial dendron-like ionizable lipid library extends the chemical diversity of ionizable lipids for nucleic acid delivery applications.

2.2. Structure−Activity Relationship (SAR) of Dendron-like LNP for FLuc mRNA Delivery In Vitro. We subsequently explored the structure−activity relationship (SAR) of dendron-like ionizable lipids for mRNA delivery in vitro. Dendron-like LNPs encapsulating FLuc mRNA were used to transfect HeLa cells, a cell line shown to be conducive to high-throughput in vitro screening of LNP formulations in previous studies.[46,47,50] Dendron-like LNPs were formulated by mixing an ethanol phase containing dendron-like lipids, DOPE, cholesterol, and C14PEG2K (35:16:46.5:2.5, molar ratio) and an aqueous phase containing FLuc mRNA via a microfluidic mixing approach (Figure 2a). Dendron-like LNPs were characterized by particle size, polydispersity index (PDI), zeta potential, and mRNA encapsulation efficiency.[14,48] The hydrodynamic diameter for all dendron-like LNP formulations ranged from 70 to 150 nm, as determined by intensity measurements using dynamic light scattering (DLS) (Tables S1−S3). Cryo-transmission electron microscopy (cryo-TEM) showed a uniform solid core morphology in a representative dendron-like LNP (Figure 2b,c). The majority of dendron-like LNP formulations (>80%) exhibited high monodispersity, with a PDI value less than 0.2 (Tables S1−S3). Additionally, dendron-like LNPs displayed a relatively negative surface zeta potential and high mRNA encapsulation efficiency (Tables S1−S3).

Following high-throughput in vitro screening in HeLa cells, a heat map illustrating dendron-like lipid-mediated mRNA delivery efficacy was generated (Figure 2d). To elucidate how structural parameters influenced mRNA delivery, the relative hit rate, defined as the value of the relative luminescence unit (RLU) greater than 200, was assessed. The amine number of each dendron-like lipid that influenced mRNA delivery efficacy was first investigated. Our data indicate that dendron-like lipids with five secondary amines per lipid exhibited the highest mRNA transfection with a hit rate of 12.6% across the entire library (Figure 2e). Notably, a higher number of secondary amine heads (>2) have been shown previously to facilitate endosomal escape of mRNA, leading to enhanced delivery efficacy.[51,52] Additionally, tail length and tail substitution numbers have been shown to influence mRNA delivery.[52,53] Among dendron-like lipids, a tail length of 9 and tail substitution number of 10 resulted in the highest relative hit rate (Figure 2f,g). Moreover, dendron-like lipids with branched architectures demonstrated superior mRNA delivery compared to linear and unsaturated counterparts (Figure 2h), aligning with prior studies indicating that branched tails may enhance stability and fusogenicity for mRNA delivery.[54,55] All dendron-like LNPs exhibited minimal toxicity in vitro (Figure S17). Interestingly, 14 dendron-like LNP formulations in this library outperformed the gold standard MC3 LNP in vitro (Figures 2d and S18). Thus, these 14 dendron-like LNP formulations were selected for subsequent investigation in vivo.

2.3. Dendron-like LNPs Facilitate In Vivo mRNA Delivery to the Spleen. Fourteen dendron-like LNPs were assessed for in vivo mRNA delivery in C57BL/6J mice following systemic administration of 0.1 mg/kg FLuc mRNA. After 12 h, mice were scarified, and organs (heart, liver, spleen, lungs, and kidneys) were isolated to quantify luciferase expression using an in vivo imaging system (IVIS) (Figure 3a,b). Notably, these dendron-like LNPs exhibited variable mRNA delivery to the spleen. To assess spleen-targeting specificity, the average luciferase expression of spleen/liver and spleen/lungs of the above dendron-like LNPs was calculated based on the IVIS data (Figure 3c,d). It was found that 13 out of these 14 dendron-like LNPs exhibited higher luciferase expression in the spleen compared to the liver (Figure 3c). Meanwhile, we synthesized 14 ionizable lipid analogs featuring only one alkyl chain in each tail and evaluated in vivo mRNA delivery (Figures S19 and S20). These ionizable lipid analogs mediated robust mRNA delivery to the liver rather than the spleen (Figure S19a,b). Only 2 out of the 14 counterpart lipids exhibited higher luciferase expression in the spleen compared to that in the liver (Figure S19c). We also investigated the correlation between LNP size (with and without dendron-like design) and spleen delivery efficacy, observing only a weak relationship between LNP size and spleen-tropic activity (Figure S20), in accordance with previous studies.[19,56] These findings underscore the importance of dendron-like designs of ionizable lipids in facilitating mRNA delivery to the spleen.

We further investigated the influence of different chemical structures on spleen-tropic mRNA delivery. Initially, the importance of the amine number was evaluated by analyzing the delivery efficacy of dendron-like ionizable lipids. An amine number of 5 mediated the most potent mRNA delivery to the spleen (Figure 3e), suggesting that a higher amine number in the lipids potentially increases spleen-tropic delivery.[19,57] Additionally, a tail length of 9 resulted in more potent expression in the spleen (Figure 3f), whereas both longer and shorter tails generally demonstrated lower levels of mRNA delivery to the spleen. Furthermore, a tail substitution number of 5 with branched tail morphology led to enhanced mRNA delivery to the spleen (Figure 3g,h). Collectively, these results highlight that the chemical structure of dendron-like ionizable lipids influences spleen-tropic mRNA delivery.

Based on these investigations, 18−2−9b2, composed of five secondary amines and 10 multiarmed degradable tails with a branched architecture, demonstrated the most efficient spleen-specific mRNA delivery (Figure S21). Although 15−2−9b and 18−2−11 exhibited greater luminescence intensity in the spleen than the 18−2−9b2 LNP, they also showed higher transfection in the liver and lungs, indicating lower specificity for the spleen. Following the analysis of both the spleen delivery efficacy and specificity, 18−2−9b2 LNP was selected for further consideration.

2.4. Endogenous Targeting Potential of Dendron-like LNPs for Spleen-Tropic Delivery. We next investigated the potential mechanism of the dendron-like design facilitating spleen-tropic delivery. First, the pK_a of LNP may influence targeted mRNA delivery to the spleen.[19,58] To better compare the results, an ionizable lipid analog without a dendron-like design, 18−1−9b2, was used (Figure S22). The pK_a value of 18−1−9b2 was found to be 6.20, consistent with previous studies indicating pK_a values between 6 and 7 for potent nucleic acid delivery to the liver (Figure S23a).[23] Conversely, the pK_a of 18−2−9b2 was 5.65, deviating from the established pK_a characteristics associated with the 18PA-based SORT spleen LNP (pK_a ranging from 4 to 5) for the mRNA delivery

https://doi.org/10.1021/jacs.4c10265
J. Am. Chem. Soc. XXXX, XXX, XXX−XXX

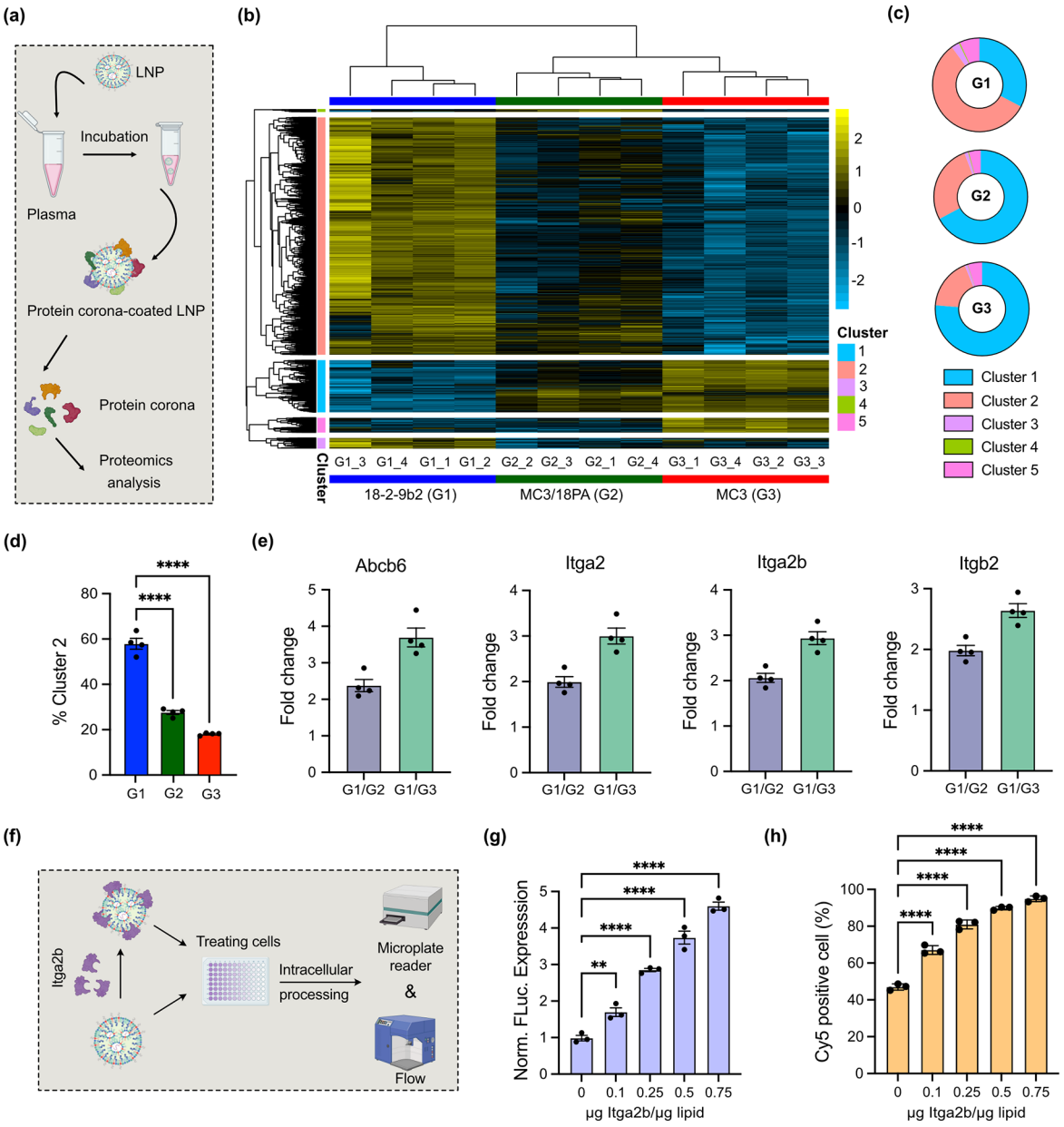

Figure 4. Proteomics analysis of protein corona bound to the LNP surface. (a) Schematic illustration of the experimental process of protein corona adsorption on the LNP for subsequent proteomics analysis. (b) Heatmap of different clusters in the protein corona between 18-2-9b2, MC3/18PA, and MC3-treated groups (n = 4). Pie chart (c) and proportion (d) of Cluster 2 in different LNP-treated groups. (e) Representative enhanced fold change of proteins in Cluster 2 between different LNP-treated groups. (f) Schematic illustration of endogenous protein adsorption on LNP-mediated intracellular processing of mRNA delivery. 18−2−9b2 LNPs were pre-coated with Itga2b and used to treat RAW264.7 cells. Luciferase expression was used to evaluate mRNA transfection (g), while flow cytometry was used to evaluate intracellular uptake of Cy5-tagged mRNA-LNP (h). Normalized luciferase expression is reported as the mean ± SEM (n = 3 biological replicates). Statistical significance in (d), (g), and (h) was calculated using one-way analysis of variance (ANOVA), followed by Dunnett's multiple comparison test. $^{**}P < 0.01$; $^{***}P < 0.001$; $^{****}P < 0.0001$.

to the spleen (Figure S23b).[23] These results suggest that the pk_a of LNPs represents only one facet of the complicated landscape governing spleen-tropic mRNA delivery activity.

Therefore, we further explored the endogenous targeting potential of 18−2−9b2 LNPs by assessing the protein corona ex vivo via mass spectrometry-based proteomics (Figures 4a and S24−S26). We noted a significant enhancement of Cluster 2 in the corona bound to the 18−2−9b2 LNP (57.3%), which is 3.23-fold and 2.11-fold enhancement compared to MC3 and MC3/18PA groups, respectively (Figure 4b−d). A further Gene Ontology (GO) enrichment analysis of Cluster 2 showed that the 18−2−9b2 LNP-treated group exhibited an increase in proteins responsible for various cellular processes, such as hematopoietic progenitor cell differentiation, transporter activity, and transmembrane transporter activity (Figure S27). These processes influence the efficacy, targeting, and intracellular processing for LNP-mediated delivery to the spleen.[23,59]

We further selected and analyzed representative proteins in Cluster 2, which are highly abundant in the corona. It was shown that the amount of Abcb6, Itga2, Itga2b, and Itgb2 in the corona of the 18−2−9b2 LNP treatment group increased

https://doi.org/10.1021/jacs.4c10265
J. Am. Chem. Soc. XXXX, XXX, XXX−XXX

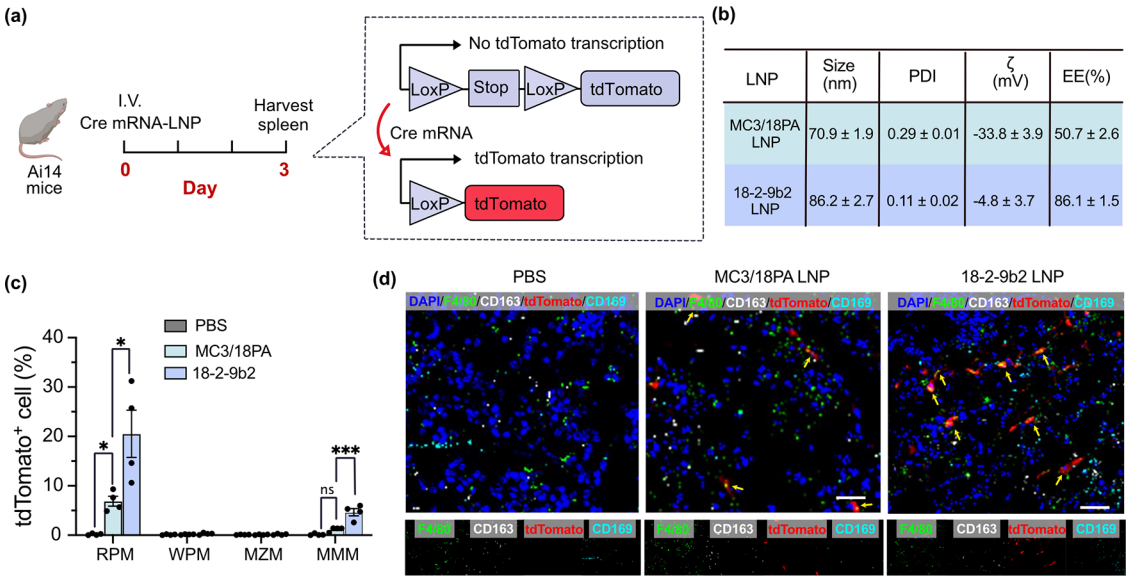

Figure 5. 18−2−9b2 LNP-mediated in vivo mRNA delivery to splenic macrophages. (a) Ai14 mice were treated with 18−2−9b2 or MC3/18PA LNP encapsulating Cre mRNA 3 days prior to analysis (0.3 mg/kg). Spleens were digested and stained for quantifying cell populations for tdTomato$^+$ expression. PBS was injected as a negative control. (b) Characterization of 18−2−9b2 and MC3/18PA LNPs. (c) Proportion of tdTomato$^+$ macrophage cell types in the spleen assessed by flow cytometry. RPM: red pulp macrophage; WPM: white pulp macrophage; MZM: marginal zone macrophage; MMM: marginal metallophilic macrophage. (d) Representative immunostaining demonstrating signal overlap between tdTomato$^+$ cells and macrophage markers (yellow arrow). DAPI was used for nuclear staining. F4/80 was used for macrophage staining. CD163 was used for RPM staining. CD169 was used for MMM staining. Statistical significance in (c) was calculated using one-way analysis of variance (ANOVA), followed by Dunnett's multiple comparison test. *P < 0.05; ***P < 0.001. Data are presented as mean ± s.e.m. (n = 4 mice).

2−5 times compared to these in MC3 and MC3/18PA LNP-treated groups (Figure 4e). Additionally, well-identified proteins like apolipoprotein E (ApoE, liver-directed nanoparticle delivery) and vitronectin (Vtn, lung-directed nanoparticle delivery) were significantly decreased in the corona of the 18−2−9b2 LNP treated group, consistent with previous studies (Figure S28).[15,21,23] Specifically, Itga2b is predominantly expressed on the surface of platelets and megakaryocytes; consequently, nanoparticles that interact with Itga2b may be preferentially directed to the spleen due to its rich platelet content.[60]

Moreover, we preincubated the 18−2−9b2 LNP with Itga2b to evaluate the effect of protein adsorption on luciferase expression and intracellular uptake in RAW264.7 cells, which share many characteristics with splenic macrophages and serve as a useful model for studying their response to nanoparticles (Figure 4f). We observed a 1.5−4.6 fold improvement in luciferase expression across all amounts of protein tested (Figure 4g) and significantly higher intracellular uptake of Cy5-tagged mRNA compared to uncoated LNPs (Figure 4h). Collectively, these results demonstrate that endogenous targeting may act as a potential mechanism for dendron-like design in facilitating mRNA delivery to the spleen.

2.5. 18−2−9b2 LNP Mediates mRNA Delivery to Splenic Macrophages. Having demonstrated that 18−2−9b2 LNP facilitates targeted mRNA delivery to the spleen, we next evaluated its ability to transfect specific cell types within the spleen. We used an Ai14 (constitutive loxP-STOP-loxP-tdTomato) reporter mouse model, which has been widely used for organ-specific gene editing studies.[19,22,34] LNP-mediated intracellular delivery of Cre recombinase mRNA in this model deletes a flanking stop cassette, leading to tdTomato fluorescence expression within the transfected cell (Figure 5a).[19,22] To benchmark the performance of our lead 18−2−9b2 LNP, a gold standard spleen-tropic MC3/18PA LNP was formulated as a positive control (Figure 5b).[22,23,30] Following a single systemic administration of 0.3 mg/kg Cre mRNA using the 18−2−9b2 LNP, effective spleen gene modulation was observed 3 days postadministration (Figures 5c and S29). In particular, we observed transfection of 20.5% of red pulp macrophages (RPM) and 4.6% of marginal metallophilic macrophage (MMM), representing a 3.0-fold and 3.8-fold improved editing efficacy compared to MC3/18PA LNP, respectively. Interestingly, we did not observe editing of other immune cell types including dendritic cells (DCs), T cells, and B cells in the spleen, which might be due to the relatively suboptimal delivery efficacy of 18−2−9b2 LNP and protocol optimization of MC3/18PA LNP (Figure S30).[61] Immunostaining of tdTomato$^+$ cells further validated the enhanced performance of 18−2−9b2 LNPs relative to that of MC3/18PA LNPs (Figure 5d). Importantly, the 18−2−9b2 LNP exhibited minimal in vivo toxicity, as evidenced by tissue section histology (Figure S31).

Specifically, red pulp macrophages (RPM), localizing in the splenic red pulp, play a crucial role in the maintenance of blood homeostasis by actively phagocytosing injured and senescent erythrocytes and blood-borne particles.[62−64] RPM accumulate large amounts of heme within their cytoplasm, and the transcription factor Spic has been reported to specifically regulate RPM development.[63,64] Heme promotes degradation of the transcriptional repressor BTB domain and CNC homologue 1 (BACH1), thereby reversing the repression of Spic by BACH1 (Figure 6a).[64] Utilizing a Spic-GFP transgene mouse model,[64,65] where the expression of Spic is inversely correlated with BACH1 and is easily quantifiable by GFP intensity in the RPM, we demonstrated the potential of the 18−2−9b2 LNP for therapeutic mRNA delivery to the spleen. The 18−2−9b2 LNP encapsulating BACH1 mRNA was

https://doi.org/10.1021/jacs.4c10265
J. Am. Chem. Soc. XXXX, XXX, XXX−XXX

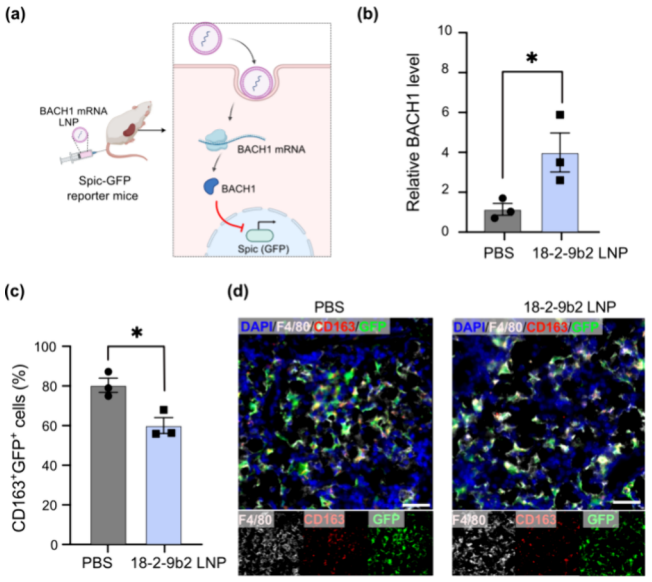

Figure 6. 18−2−9b2 LNP-mediated in vivo BACH1 mRNA delivery to the spleen of Spic-GFP reporter mice. (a) 18−2−9b2 LNP-mediated BACH1 expression can repress the expression of Spic, leading to the downregulation of the GFP signal in a Spic-GFP reporter mice model. LNP was systemically administered into mice at a dosage of 1.0 mg/kg. (b) BACH1 level in sorted RPM was evaluated by quantitative PCR. (c) Proportion of GFP^+ RPM assessed by flow cytometry. (d) Representative immunostaining demonstrating decreased GFP signal after BACH1 mRNA delivery. DAPI was used for nuclear staining. F4/80 was used for macrophage staining. CD163 was used for RPM staining. Statistical significance in (b) and (c) was calculated using a Student's *t* test with unpaired design. $^*P < 0.05$. Data are presented as mean ± s.e.m. (n = 3 mice).

systemically injected to Spic-GFP mice, and after 48h, mice were sacrificed, and the spleen was isolated for further evaluation. Quantitative PCR (qPCR) was employed to assess the delivery of BACH1 to RPM (Figure 6b). In comparison to PBS-treated mice, the expression of BACH1 in 18−2−9b2 LNP-treated mice repressed the expression of Spic, leading to the downregulation of GFP signal observed through flow cytometry and immunostaining (Figures 6c,d and S32). Collectively, these data demonstrate that the development of 18−2−9b2 LNP with a dendron-like structure can facilitate targeted mRNA delivery to splenic RPM, and the delivery of therapeutic BACH1 mRNA using this platform holds potential to regulate transcriptional factors within splenic RPM.

3. CONCLUSIONS

In summary, we developed a straightforward approach to construct a library of dendron-like degradable ionizable lipids with tailed dendron-like architectures that can be formulated into dendron-like LNPs. Following high-throughput in vitro screening, we identified 14 dendron-like LNPs demonstrating transfection efficacy superior to that of the gold standard MC3 LNP formulation. These selected LNPs were further validated for facilitating mRNA delivery to the spleen through systemic administration in vivo, in comparison with ionizable lipid analogs lacking dendron-like structures. The lead dendron-like LNP, 18−2−9b2, adsorbs a series of hematopoietic and transmembrane transporter-related proteins in the serum, potentially directing its spleen tropism. Furthermore, 18−2−9b2 LNP encapsulating Cre mRNA demonstrates targeting of spleen red pulp macrophages and marginal metallophilic macrophage in the Ai14 mice model, outperforming a spleen-tropic MC3/18PA LNP system. This lead dendron-like LNP was then used for delivering BACH1 mRNA in Spic-GFP reporter mice, wherein the expression of BACH1 effectively repressed the Spic-GFP signal, highlighting the potential for regulating transcriptional factors through mRNA delivery. Our innovative design of dendron-like degradable ionizable lipids holds potential promise for targeted mRNA therapeutics, regenerative medicine, and gene editing applications in the spleen. The design of dendron-like lipids may open new avenues to construct next-generation LNP formulations for extrahepatic mRNA delivery.

■ ASSOCIATED CONTENT

Supporting Information

The Supporting Information is available free of charge at https://pubs.acs.org/doi/10.1021/jacs.4c10265.

Materials and instruments; details of synthetic procedures; lipid nanoparticles formulation and characterization; high-throughput in vitro screening; cell viability; in vivo luciferase mRNA delivery of dendron-like and their counterpart LNPs; Cre mRNA delivery to Ai14 mice; BACH1 mRNA delivery to Spic-GFP reporter mice; proteomics analysis; H&E staining; sequence of BACH1 mRNA; and markers in each cluster from proteomics test (PDF)

■ AUTHOR INFORMATION

Corresponding Author

Michael J. Mitchell − *Department of Bioengineering, Penn Institute for RNA Innovation, Perelman School of Medicine, Abramson Cancer Center, Perelman School of Medicine, Institute for Immunology, Perelman School of Medicine, and Institute for Regenerative Medicine, Perelman School of Medicine, University of Pennsylvania, Philadelphia, Pennsylvania 19104, United States; Cardiovascular Institute, Perelman School of Medicine, University of Pennsylvania, Philadelphia, Pennsylvania 19014, United States;* orcid.org/0000-0002-3628-2244; Email: mjmitch@seas.upenn.edu

Authors

Lulu Xue − *Department of Bioengineering, University of Pennsylvania, Philadelphia, Pennsylvania 19104, United States;* orcid.org/0000-0001-5719-1336

Xinhong Xiong − *Yangtze Delta Region Institute (Huzhou), University of Electronic Science and Technology of China, Huzhou, Zhejiang 313001, China*

Gan Zhao − *Department of Biomedical Sciences, School of Veterinary Medicine, University of Pennsylvania, Philadelphia, Pennsylvania 19104, United States*

William Molina-Arocho − *Department of Pathology and Laboratory Medicine, Perelman School of Medicine, University of Pennsylvania, Philadelphia, Pennsylvania 19104, United States*

Rohan Palanki − *Department of Bioengineering, University of Pennsylvania, Philadelphia, Pennsylvania 19104, United States;* orcid.org/0000-0001-5168-5634

Zebin Xiao − *Department of Biomedical Sciences, School of Veterinary Medicine, University of Pennsylvania, Philadelphia, Pennsylvania 19104, United States*

https://doi.org/10.1021/jacs.4c10265
J. Am. Chem. Soc. XXXX, XXX, XXX−XXX

Xuexiang Han − *Department of Bioengineering, University of Pennsylvania, Philadelphia, Pennsylvania 19104, United States*
Il-Chul Yoon − *Department of Bioengineering and Department of Materials Science and Engineering, University of Pennsylvania, Philadelphia, Pennsylvania 19104, United States*
Christian G. Figueroa-Espada − *Department of Bioengineering, University of Pennsylvania, Philadelphia, Pennsylvania 19104, United States;* orcid.org/0000-0003-2700-7678
Junchao Xu − *Department of Bioengineering, University of Pennsylvania, Philadelphia, Pennsylvania 19104, United States*
Ningqiang Gong − *Department of Bioengineering, University of Pennsylvania, Philadelphia, Pennsylvania 19104, United States;* orcid.org/0000-0002-9444-8505
Qiangqiang Shi − *Department of Bioengineering, University of Pennsylvania, Philadelphia, Pennsylvania 19104, United States*
Qinyuan Chen − *School of Dental Medicine, University of Pennsylvania, Philadelphia, Pennsylvania 19104, United States*
Mohamad-Gabriel Alameh − *Department of Medicine and Penn Institute for RNA Innovation, Perelman School of Medicine, University of Pennsylvania, Philadelphia, Pennsylvania 19104, United States;* orcid.org/0000-0002-5672-6930
Andrew E. Vaughan − *Department of Biomedical Sciences, School of Veterinary Medicine, University of Pennsylvania, Philadelphia, Pennsylvania 19104, United States*
Malay Haldar − *Department of Pathology and Laboratory Medicine, Perelman School of Medicine, University of Pennsylvania, Philadelphia, Pennsylvania 19104, United States*
Karin Wang − *Department of Bioengineering, Temple University, Philadelphia, Pennsylvania 19122, United States;* orcid.org/0000-0001-7812-2583
Drew Weissman − *Department of Medicine and Penn Institute for RNA Innovation, Perelman School of Medicine, University of Pennsylvania, Philadelphia, Pennsylvania 19104, United States;* orcid.org/0000-0002-1501-6510

Complete contact information is available at: https://pubs.acs.org/10.1021/jacs.4c10265

Funding

NIH Director's New Innovator Award (DP2 TR002776), Burroughs Wellcome Fund Career Award at the Scientific Interface (CASI), grant from the US National Science Foundation CAREER Award (CBET-2145491), an American Cancer Society Research Grant (RSG-22-122-01-ET), and the National Institutes of Health (NICHD R01 HD115877).

Notes

The authors declare the following competing financial interest(s): L.X. and M.J.M. have filed a patent application based on this research. D.W. is named on patents that describe the use of nucleoside-modified mRNA as a platform to deliver therapeutic proteins and vaccines. M.J.M., D.W. and M.G.A. are also named on patents describing the use of lipid nanoparticles, and lipid compositions for nucleic acid delivery. The other authors declare no competing interests.

■ ACKNOWLEDGMENTS

M.J.M. acknowledges support from a US National Institutes of Health (NIH) Director's New Innovator Award (DP2 TR002776), a Burroughs Wellcome Fund Career Award at the Scientific Interface (CASI), an American Cancer Society Research Grant (RSG-22-122-01-ET), a US National Science Foundation CAREER Award (CBET-2145491), and the National Institutes of Health (NICHD R01 HD115877). R.P. was supported by an NIH F30 fellowship (F30HL162465-01A1). C.G.F.-E. was supported by a National Science Foundation Graduate Research Fellowship (DGE 1845298), a GEM Fellowship, and the NCI Predoc to Postdoc Transition Award (F99 CA284294). Z.X. was supported by CRI Irvington fellowship (Grant#: CRI4168) from Cancer Research Institute. We thank Penn Proteomic Core (CHOP) for the whole proteome data analysis. We thank BioRender for providing a platform to create the cartoons and schematics used in the figures.

■ ABBREVIATIONS

messenger RNA, mRNA; RPM, red pulp macrophage; WPM, white pulp macrophage; MZM, marginal zone macrophage; MMM, marginal metallophilic macrophage; BACH1, BTB domain and CNC homologue 1

■ REFERENCES

(1) Yin, H.; Kauffman, K. J.; Anderson, D. G. Delivery technologies for genome editing. *Nat. Rev. Drug. Discovery* **2017**, *16* (6), 387−399.
(2) Chaudhary, N.; Weissman, D.; Whitehead, K. A. mRNA vaccines for infectious diseases: principles, delivery and clinical translation. *Nat. Rev. Drug. Discovery* **2021**, *20* (11), 817−838.
(3) Sahin, U.; Kariko, K.; Tureci, O. mRNA-based therapeutics–developing a new class of drugs. *Nat. Rev. Drug. Discovery* **2014**, *13* (10), 759−780.
(4) Pastor, F.; Berraondo, P.; Etxeberria, I.; Frederick, J.; Sahin, U.; Gilboa, E.; Melero, I. An RNA toolbox for cancer immunotherapy. *Nat. Rev. Drug. Discovery* **2018**, *17* (10), 751−767.
(5) LoPresti, S. T.; Arral, M. L.; Chaudhary, N.; Whitehead, K. A. The replacement of helper lipids with charged alternatives in lipid nanoparticles facilitates targeted mRNA delivery to the spleen and lungs. *J. Controlled Release* **2022**, *345*, 819−831.
(6) Eygeris, Y.; Gupta, M.; Kim, J.; Sahay, G. Chemistry of Lipid Nanoparticles for RNA Delivery. *Acc. Chem. Res.* **2022**, *55* (1), 2−12.
(7) Hou, X.; Zaks, T.; Langer, R.; Dong, Y. Lipid nanoparticles for mRNA delivery. *Nat. Rev. Mater.* **2021**, *6* (12), 1078−1094.
(8) Mendes, B. B.; Conniot, J.; Avital, A.; Yao, D.; Jiang, X.; Zhou, X.; Sharf-Pauker, N.; Xiao, Y.; Adir, O.; Liang, H.; Shi, J.; Schroeder, A.; Conde, J. Nanodelivery of nucleic acids. *Nat. Rev. Methods Primers* **2022**, *2*, 24.
(9) Hajj, K. A.; Whitehead, K. A. Tools for translation: non-viral materials for therapeutic mRNA delivery. *Nat. Rev. Mater.* **2017**, *2*, 17056.
(10) Chung, J. Y.; Thone, M. N.; Kwon, Y. J. COVID-19 vaccines: The status and perspectives in delivery points of view. *Adv. Drug. Delivery Rev.* **2021**, *170*, 1−25.
(11) Huang, X.; Kong, N.; Zhang, X.; Cao, Y.; Langer, R.; Tao, W. The landscape of mRNA nanomedicine. *Nat. Med.* **2022**, *28* (11), 2273−2287.
(12) Naddaf, M. First trial of "base editing" in humans lowers cholesterol - but raises safety concerns. *Nature* **2023**, *623* (7988), 671−672.
(13) Gillmore, J. D.; Gane, E.; Taubel, J.; Kao, J.; Fontana, M.; Maitland, M. L.; Seitzer, J.; O'Connell, D.; Walsh, K. R.; Wood, K.; Phillips, J.; Xu, Y.; Amaral, A.; Boyd, A. P.; Cehelsky, J. E.; Mckee, M. D.; Schiermeier, A.; Harari, O.; Chir, B.; Murphy, A.; Kyratsous, C. A.; Zambrowicz, B.; Soltys, R.; Gutstein, D.; Leonard, J.; Sepp-

Lorenzino, L.; Lebwohl, D. CRISPR-Cas9 in vivo gene editing for transthyretin amyloidosis. *N. Engl. J. Med.* **2021**, *385* (6), 493−502.
(14) Xue, L.; Gong, N.; Shepherd, S. J.; Xiong, X.; Liao, X.; Han, X.; Zhao, G.; Song, C.; Huang, X.; Zhang, H.; Padilla, M. S.; Qin, J.; Shi, Y.; Alameh, M. G.; Pochan, D. J.; Wang, K.; Long, F.; Weissman, D.; Mitchell, M. J. Rational design of bisphosphonate lipid-like materials for mRNA delivery to the bone microenvironment. *J. Am. Chem. Soc.* **2022**, *144* (22), 9926−9937.
(15) Qiu, M.; Tang, Y.; Chen, J.; Muriph, R.; Ye, Z.; Huang, C.; Evans, J.; Henske, E. P.; Xu, Q. Lung-selective mRNA delivery of synthetic lipid nanoparticles for the treatment of pulmonary lymphangioleiomyomatosis. *Proc. Natl. Acad. Sci. U S A* **2022**, *119* (8), No. e2116271119.
(16) Herrera-Barrera, M.; Ryals, R. C.; Gautam, M.; Jozic, A.; Landry, M.; Korzun, T.; Gupta, M.; Acosta, C.; Stoddard, J.; Reynaga, R.; Tschetter, W.; Jacomino, N.; Taratula, O.; Sun, C.; Lauer, A. K.; Neuringer, M.; Sahay, G. Peptide-guided lipid nanoparticles deliver mRNA to the neural retina of rodents and nonhuman primates. *Sci. Adv.* **2023**, *9* (2), No. eadd4623.
(17) Han, X.; Alameh, M. G.; Butowska, K.; Knox, J. J.; Lundgreen, K.; Ghattas, M.; Gong, N.; Xue, L.; Xu, Y.; Lavertu, M.; Bates, P.; Xu, J.; Nie, G.; Zhong, Y.; Weissman, D.; Mitchell, M. J. Adjuvant lipidoid-substituted lipid nanoparticles augment the immunogenicity of SARS-CoV-2 mRNA vaccines. *Nat. Nanotechnol.* **2023**, *18* (9), 1105−1114.
(18) Tilstra, G.; Couture-Senecal, J.; Lau, Y. M. A.; Manning, A. M.; Wong, D. S. M.; Janaeska, W. W.; Wuraola, T. A.; Pang, J.; Khan, O. F. Iterative design of ionizable lipids for intramuscular mRNA delivery. *J. Am. Chem. Soc.* **2023**, *145* (4), 2294−2304.
(19) Ni, H.; Hatit, M. Z. C.; Zhao, K.; Loughrey, D.; Lokugamage, M. P.; Peck, H. E.; Cid, A. D.; Muralidharan, A.; Kim, Y.; Santangelo, P. J.; Dahlman, J. E. Piperazine-derived lipid nanoparticles deliver mRNA to immune cells in vivo. *Nat. Commun.* **2022**, *13* (1), 4766.
(20) Zhao, G.; Xue, L.; Weiner, A. I.; Gong, N.; Adams-Tzivelekidis, S.; Wong, J.; Gentile, M. E.; Nottingham, A. N.; Basil, M. C.; Lin, S. M.; Niethamer, T. L.; Diamound, J. M.; Bermudez, C. A.; Cantu, E.; Han, X.; Cao, Y.; Alameh, M. G.; Weissman, D.; Morrisey, E. E.; Mitchell, M. J.; Vaughan, A. E. TGF-βR2 signaling coordinates pulmonary vascular repair after viral injury in mice and human tissue. *Sci. Transl. Med.* **2024**, *16* (7), No. eadg6229.
(21) Xue, L.; Zhao, G.; Gong, N.; Han, X.; Shepherd, S. J.; Xiong, X.; Xiao, Z.; Palanki, R.; Xu, J.; Swingle, K. L.; Warzecha, C. C.; El-Mayta, R.; Chowdhary, V.; Yoon, C.; Xu, J.; Cui, J.; Shi, Y.; Alameh, M. G.; Wang, K.; Wang, L.; Pochan, D. J.; Weissman, D.; Vaughan, A. E.; Wilson, J. M.; Mitchell, M. J. Combinatorial design of siloxane-incorporated lipid nanoparticles augments intracellular processing for tissue-specific mRNA therapeutic delivery. *Nat. Nanotechnol.* **2024**. DOI: DOI: 10.1038/s41565-024-01747-6.
(22) Cheng, Q.; Wei, T.; Farbiak, L.; Johnson, L. T.; Dilliard, S. A.; Siegwart, D. J. Selective organ targeting (SORT) nanoparticles for tissue-specific mRNA delivery and CRISPR-Cas gene editing. *Nat. Nanotechnol.* **2020**, *15* (4), 313−320.
(23) Dilliard, S. A.; Cheng, Q.; Siegwart, D. J. On the mechanism of tissue-specific mRNA delivery by selective organ targeting nanoparticles. *Proc. Natl. Acad. Sci. U. S. A.* **2021**, *118* (5), No. e2109256118.
(24) Alexandre, Y. O.; Mueller, S. N. Splenic stromal niches in homeostasis and immunity. *Nat. Rev. Immunol.* **2023**, *23* (11), 705−719.
(25) Bronte, V.; Pittet, M. J. The spleen in local and systemic regulation of immunity. *Immunity* **2013**, *39* (5), 806−818.
(26) Mebius, R. E.; Kraal, G. Structure and function of the spleen. *Nat. Rev. Immunol.* **2005**, *5* (8), 606−616.
(27) Porosk, L.; Hark, H. H.; Arukuusk, P.; Haljasorg, U.; Peterson, P.; Kurrikoff, K. The development of cell-penetrating peptides for efficient and selective in vivo expression of mRNA in spleen tissue. *Pharmaceutics* **2023**, *15* (3), 952.
(28) Dilliard, S. A.; Siegwart, D. J. Passive, active and endogenous organ-targeted lipid and polymer nanoparticles for delivery of genetic drugs. *Nat. Rev. Mater.* **2023**, *8* (4), 282−300.
(29) Kimura, S.; Khalil, I. A.; Elewa, Y. H. A.; Harashima, H. Spleen selective enhancement of transfection activities of plasmid DNA driven by octaarginine and an ionizable lipid and its implications for cancer immunization. *J. Controlled Release* **2019**, *313*, 70−79.
(30) Alvarez-Benedicto, E.; Tian, Z.; Chatterjee, S.; Orlando, D.; Kim, M.; Guerrero, E. D.; Wang, X.; Siegwart, D. J. Spleen SORT LNP generated in situ CAR T cells extend survival in a mouse model of lymphoreplete B Cell lymphoma. *Angew. Chem., Int. Ed.* **2023**, *62* (44), No. e202310395.
(31) Liu, S.; Cheng, Q.; Wei, T.; Yu, X.; Johnson, L. T.; Farbiak, L.; Siegwart, D. J. Membrane-destabilizing ionizable phospholipids for organ-selective mRNA delivery and CRISPR-Cas gene editing. *Nat. Mater.* **2021**, *20* (5), 701−710.
(32) Liu, S.; Wang, X.; Yu, X.; Cheng, Q.; Johnson, L. T.; Chatterjee, S.; Zhang, D.; Lee, S. M.; Sun, Y.; Lin, T. C.; Liu, J. L.; Siegwart, D. J. Zwitterionic phospholipidation of cationic polymers facilitates systemic mRNA delivery to spleen and lymph nodes. *J. Am. Chem. Soc.* **2021**, *143* (50), 21321−21330.
(33) Pan, L.; Zhang, L.; Deng, W.; Lou, J.; Gao, X.; Lou, X.; Liu, Y.; Yao, X.; Sheng, Y.; Yan, Y.; Ni, C.; Wang, M.; Tian, C.; Wang, F.; Qin, Z. Spleen-selective co-delivery of mRNA and TLR4 agonist-loaded LNPs for synergistic immunostimulation and Th1 immune responses. *J. Controlled Release* **2023**, *357*, 133−148.
(34) Zhao, X.; Chen, J.; Qiu, M.; Li, Y.; Glass, Z.; Xu, Q. Imidazole-based synthetic lipidoids for in vivo mRNA delivery into primary T lymphocytes. *Angew. Chem., Int. Ed.* **2020**, *59* (45), 20083−20089.
(35) Zhang, R.; Shao, S.; Piao, Y.; Xiang, J.; Wei, X.; Zhang, Z.; Zhou, Z.; Tang, J.; Qiu, N.; Xu, X.; Liu, Y.; Shen, Y. Esterase-labile quaternium lipidoid enabling improved mRNA-LNP stability and spleen-Selective mRNA transfection. *Adv. Mater.* **2023**, *35* (46), No. e2303614.
(36) Ben-Akiva, E.; Karlsson, J.; Hemmati, S.; Yu, H.; Tzeng, S. Y.; Pardoll, D. M.; Green, J. J. Biodegradable lipophilic polymeric mRNA nanoparticles for ligand-free targeting of splenic dendritic cells for cancer vaccination. *Proc. Natl. Acad. Sci. U. S. A.* **2023**, *120* (26), No. e2301606120.
(37) Fenton, O. S.; Kauffman, K. J.; Kaczmarek, J. C.; McClellan, R. L.; Jhunjhunwala, S.; Tibbitt, M. W.; Zeng, M. D.; Appel, E. A.; Dorkin, J. R.; Mir, F. F.; Yang, J. H.; Oberli, M. A.; Heartlein, M. W.; DeRosa, F.; Langer, R.; Anderson, D. G. Synthesis and biological evaluation of ionizable lipid materials for the in vivo delivery of messenger RNA to B lymphocytes. *Adv. Mater.* **2017**, *29* (33), No. 1606944.
(38) He, Z.; Le, Z.; Shi, Y.; Liu, L.; Liu, Z.; Chen, Y. A Multidimensional approach to modulating ionizable lipids for high-performing and organ-selective mRNA delivery. *Angew. Chem., Int. Ed.* **2023**, *62* (43), No. e202310401.
(39) Mullner, M. Molecular polymer bottlebrushes in nanomedicine: therapeutic and diagnostic applications. *Chem. Commun.* **2022**, *58* (38), 5683−5716.
(40) Sharma, A.; Pande, P. P. Recent advancement in comb-like polymers: a review. *J. Polym. Mater.* **2019**, *36* (2), 175−194.
(41) Verduzco, R.; Li, X.; Pesek, S. L.; Stein, G. E. Structure, function, self-assembly, and applications of bottlebrush copolymers. *Chem. Soc. Rev.* **2015**, *44* (8), 2405−2420.
(42) Gallot, B. Comb-like and block liquid crystalline polymers for biological applications. *Prog. Polym. Sci.* **1996**, *21* (6), 1035−1088.
(43) Lin, Y. L.; Jiang, G.; Birrell, L. K.; El-Sayed, M. E. Degradable, pH-sensitive, membrane-destabilizing, comb-like polymers for intracellular delivery of nucleic acids. *Biomaterials* **2010**, *31* (27), 7150−7166.
(44) Wang, D.; Wang, Q.; Wang, Y.; Chen, P.; Lu, X.; Jia, F.; Sun, Y.; Sun, T.; Zhang, L.; Che, F.; He, J.; Lian, L.; Morano, G.; Shen, M.; Ren, M.; Dong, S. S.; Zhao, J. J.; Zhang, K. Targeting oncogenic KRAS with molecular brush-conjugated antisense oligonucleotides. *Proc. Natl. Acad. Sci. U S A* **2022**, *119* (29), No. e2113180119.

(45) Wang, D.; Lin, J.; Jia, F.; Tan, X.; Wang, Y.; Sun, X.; Cao, X.; Che, F.; Lu, H.; Gao, X.; Shimkonis, J. C.; Nyoni, Z.; Lu, X.; Zhang, K. Bottlebrush-architectured poly(ethylene glycol) as an efficient vector for RNA interference in vivo. *Sci. Adv.* **2019**, *5* (2), No. eaav9322.
(46) Akinc, A.; Zumbuehl, A.; Goldberg, M.; Leshchiner, E. S.; Busini, V.; Hossain, N.; Bacallado, S. A.; Nguyen, D. N.; Fuller, J.; Alvarez, R.; Borodovsky, A.; Borland, T.; Constien, R.; de Fougerolles, A.; Dorkin, J. R.; Jayaprakash, K. N.; Jayaraman, M.; Jon, M.; Koteliansky, V.; Manoharan, M.; Nechev, L.; Qin, J.; Racie, T.; Raitcheva, D.; Rajeev, K. G.; Sah, D. W.; Soutschek, J.; Toudjarska, I.; Vornlocher, H. P.; Zimmermann, T. S.; Langer, R.; Anderson, D. G. A combinatorial library of lipid-like materials for delivery of RNAi therapeutics. *Nat. Biotechnol.* **2008**, *26* (5), 561−569.
(47) Semple, S. C.; Akinc, A.; Chen, J.; Sandhu, A. P.; Mui, B. L.; Cho, C. K.; Sah, D. W.; Stebbing, D.; Crosley, E. J.; Yaworski, E.; Hafez, I. M.; Dorkin, J. R.; Qin, J.; Lam, K.; Rajeev, K. G.; Wong, K. F.; Jeffs, L. B.; Nechev, L.; Eisenhardt, M. L.; Jayaraman, M.; Kazem, M.; Maier, M. A.; Srinivasulu, M.; Weinstein, M. J.; Chen, Q.; Alvarez, R.; Barros, S. A.; De, S.; Klimuk, S. K.; Borland, T.; Kosovrasti, V.; Cantley, W. L.; Tam, Y. K.; Manoharan, M.; Ciufolini, M. A.; Tracy, M. A.; de Fougerolles, A.; MacLachlan, I.; Cullis, P. R.; Madden, T. D.; Hope, M. J. Rational design of cationic lipids for siRNA delivery. *Nat. Biotechnol.* **2010**, *28* (2), 172−176.
(48) Chen, D.; Love, K. T.; Chen, Y.; Eltoukhy, A. A.; Kastrup, C.; Sahay, G.; Jeon, A.; Dong, Y.; Whitehead, K. A.; Anderson, D. G. Rapid discovery of potent siRNA-containing lipid nanoparticles enabled by controlled microfluidic formulation. *J. Am. Chem. Soc.* **2012**, *134* (16), 6948−6951.
(49) Shepherd, S. J.; Warzecha, C. C.; Yadavali, S.; El-Mayta, R.; Alameh, M. G.; Wang, L.; Weissman, D.; Wilson, J. M.; Issadore, D.; Mitchell, M. J. Scalable mRNA and siRNA lipid nanoparticle production using a parallelized microfluidic device. *Nano Lett.* **2021**, *21* (13), 5671−5680.
(50) Love, K. T.; Mahon, K. P.; Levins, C. G.; Whitehead, K. A.; Querbes, W.; Dorkin, J. R.; Qin, J.; Cantley, W.; Qin, L. L.; Racie, T.; Frank-kamenetsky, M.; Yip, K. N.; Alvarez, R.; Sah, D. W.; de Fougerolles, A.; Fitzgerald, K.; Koteliansky, V.; Akinc, A.; Langer, R.; Anderson, D. G. Lipid-like materials for low-dose, in vivo gene silencing. *Proc. Natl. Acad. Sci. U S A* **2010**, *107* (5), 1864−1869.
(51) Bus, T.; Traeger, A.; Schubert, U. S. The great escape: how cationic polyplexes overcome the endosomal barrier. *J. Mater. Chem. B* **2018**, *6* (43), 6904−6918.
(52) Zhang, Y.; Sun, C.; Wang, C.; Jankovic, K. E.; Dong, Y. Lipids and lipid derivatives for RNA delivery. *Chem. Rev.* **2021**, *121* (20), 12181−12277.
(53) Sato, Y.; Hashiba, K.; Sasaki, K.; Maeki, M.; Tokeshi, M.; Harashima, H. Understanding structure-activity relationships of pH-sensitive cationic lipids facilitates the rational identification of promising lipid nanoparticles for delivering siRNAs in vivo. *J. Controlled Release* **2019**, *295*, 140−152.
(54) Hajj, K. A.; Ball, R. L.; Deluty, S. B.; Singh, S. R.; Strelkova, D.; Knapp, C. M.; Whitehead, K. A. Branched-tail lipid nanoparticles potently deliver mRNA in vivo due to enhanced ionization at endosomal pH. *Small* **2019**, *15* (6), No. e1805097.
(55) Hashiba, K.; Sato, Y.; Taguchi, M.; Sakamoto, S.; Otsu, A.; Maeda, Y.; Shishido, T.; Murakawa, M.; Okazaki, A.; Harashima, H. Branching ionizable lipids can enhance the stability, fusogenicity, and functional delivery of mRNA. *Small. Sci.* **2023**, *3* (1), 2200071.
(56) Xue, L.; Hamilton, A. G.; Zhao, G.; Xiao, Z.; El-Mayta, R.; Han, X.; Gong, N.; Xiong, X.; Xu, J.; Figueroa-Espada, C. G.; Shepherd, S. J.; Mukalel, A. J.; Alameh, M. G.; Cui, J.; Wang, K.; Vaughan, A. E.; Weissman, D.; Mitchell, M. J. High-throughput barcoding of nanoparticles identifies cationic, degradable lipid-like materials for mRNA delivery to the lungs in female preclinical models. *Nat. Commun.* **2024**, *15*, 1884.
(57) Zhang, X.; Su, K.; Wu, S.; Lin, L.; He, S.; Yan, X.; Shi, L.; Liu, S. One-component cationic lipids for systemic mRNA delivery to splenic T cells. *Angew. Chem., Int. Ed.* **2024**, *63* (26), No. e202405444.
(58) Su, K.; Shi, L.; Sheng, T.; Yan, X.; Lin, L.; Meng, C.; Wu, S.; Chen, Y.; Zhang, Y.; Wang, C.; Wang, Z.; Qiu, J.; Zhao, J.; Xu, T.; Ping, Y.; Gu, Zhen; Liu, S. Reformulating lipid nanoparticles for organ-targeted mRNA accumulation and translation. *Nat. Commun.* **2024**, *15*, 5659.
(59) Narasipura, E. A.; Fenton, O. S. Advances in non-viral mRNA delivery to the spleen. *Biomater. Sci.* **2024**, *12* (12), 3027−3044.
(60) Short, C.; Lim, H. K.; Tan, J.; O'Neill, H. C. Targeting the spleen as an alternative site for hematopoiesis. *Bioessays* **2019**, *41* (5), No. e1800234.
(61) Wang, X.; Liu, S.; Sun, Y.; Yu, X.; Lee, S. M.; Cheng, Q.; Wei, T.; Gong, J.; Robinson, J.; Zhang, D.; Lian, X.; Basak, P.; Siegwart, D. J. Preparation of selective organ-targeting (SORT) lipid nanoparticles (LNPs) using multiple technical methods for tissue-specific mRNA delivery. *Nat. Protoc.* **2023**, *18* (1), 265−291.
(62) Kurotaki, D.; Uede, T.; Tamura, T. Functions and development of red pulp macrophages. *Microbiol. Immunol.* **2015**, *59* (2), 55−62.
(63) Kohyama, M.; Ise, W.; Edelson, B. T.; Wilker, P. R.; Hildner, K.; Mejia, C.; Frazier, W. A.; Murphy, T. L.; Murphy, K. M. Role for Spi-C in the development of red pulp macrophages and splenic iron homeostasis. *Nature* **2009**, *457* (7227), 318−321.
(64) Haldar, M.; Kohyama, M.; So, A. Y.; Kc, W.; Wu, X.; Briseno, C. G.; Satpathy, A. T.; Kretzer, N. M.; Arase, H.; Rajasekaran, N. S.; Wang, L.; Egawa, T.; Igarashi, K.; Baltimore, D.; Murphy, T. L.; Murphy, K. M. Heme-mediated SPI-C induction promotes monocyte differentiation into iron-recycling macrophages. *Cell* **2014**, *156* (6), 1223−1234.
(65) Alam, Z.; Devalaraja, S.; Li, M.; To, T. K. J.; Folkert, I. W.; Mitchell-Velasquez, E.; Dang, M. T.; Young, P.; Wilbur, C. J.; Silverman, M. A.; Li, X.; Chen, Y. H.; Hernandez, P. T.; Bhattacharyya, A.; Bhattacharya, M.; Levine, M. H.; Haldar, M. Counter regulation of Spic by NF-kappaB and STAT signaling controls inflammation and iron metabolism in macrophages. *Cell. Rep.* **2020**, *31* (13), No. 107825.

https://doi.org/10.1021/jacs.4c10265
J. Am. Chem. Soc. XXXX, XXX, XXX−XXX